Journal of Electroceramics, 13, 433–442, 2004

Design and Performance of Miniaturized Piezoelectric Step-Down Transformer

KEE-JOE LIM,*[,1] SEONG-HWA KANG[2], HYUN-HOO KIM[3], JONG-SUB LEE[4] & SU-HYUN JEONG[5]

[1]*School of Electrical and Computer Engineering, Chungbuk National University, Cheongju, Chungbuk, 361-763, Korea*
[2]*Department of Industrial Safety Engineering, Chungcheong College, Cheongwon, Chungbuk, Korea*
[3]*Department of Digital Electronics, Doowon College, Ansung, Kyeonggi, Korea*
[4]*R&D Center, EMD Co., Ltd. Ipjang Myun, Cheonan, Chungnam, Korea*
[5]*Department of Electrical Engineering, Daewon Science College, Chechon, Chungbuk, Korea*

Submitted February 12, 2003; Revised March 29, 2004; Accepted July 27, 2004

Abstract. Piezoelectric transformers are expected to be small, thin and highly efficient, and which are attractive as a transformer with high power density for step down voltage. For these reasons, we have attempted to develop a step-down piezoelectric transformer for the miniaturized adaptor. we propose a piezoelectric transformer, operating in thickness extensional vibration mode for step-down voltage. This transformer consists of a multi-layered construction in the thickness direction. In order to develop the step-down piezoelectric transformers of 10 W class and turn ratio of 0.1 with high efficiency and miniaturization, the piezoelectric ceramics and piezoelectric transformer designs are estimated with a variety of characteristics. The basic composition of piezoelectric ceramics consists of ternary $yPb(Zr_xTi_{1-x})O_3 - (1-y)Pb(Mn_{1/3}Nb_{1/3}Sb_{1/3})O_3$. In the piezoelectric characteristics evaluations, at $y = 0.95$ and $x = 0.505$, the electromechanical coupling factor(k_p) is 58%, piezoelectric strain constant (d_{33}) is 270 pC/N, mechanical quality factor(Q_m) is 1520, permittivity ($\varepsilon_{33}^T/\varepsilon_0$) is 1500, and Curie temperature is 350°C. At $y = 0.90$ and $x = 0.500$, k_p is 56%, d_{33} is 250 pC/N, Q_m is 1820, $\varepsilon_{33}^T/\varepsilon_0$ is 1120, and Curie temperature is 290°C. It shows the excellent properties at morphotropic phase boundary regions. PZT-PMNS ceramic may be available for high power piezoelectric devices such as piezoelectric transformers. The design of step-down piezoelectric transformers for adaptor proposes a multi-layer structure to overcome some structural defects of conventional piezoelectric transformers. In order to design piezoelectric transformers and analyze their performances, the finite element analysis and equivalent circuit analysis method are applied. The maximum peak of gain G as a first mode for thickness extensional vibration occurs near 0.85 MHz at load resistance of 10 Ω. The peak of second mode at 1.7 MHz is 0.12 and the efficiency is 92%.

Keywords: piezoelectric transformer, PZT-PMNS, adaptor

1. Introduction

Piezoelectric transformer (so called, PT) is basically an energy converter, which transmits electrical energy through mechanical vibration, and has several inherent advantages in comparison with the wire-type electromagnetic transformers. PTs do not have winding typically and are possible to be small, thin and highly efficient, because it is not generated the electromagnetic loss including eddy-current loss and hysteresis loss, derived from the conventional wired-type transformers during high frequency operation [1]. Since C.A. Rosen proposed a piezoelectric transformer operating in length extensional vibration in 1950s, it has not been great attractive interesting and carried out vigorous studies. However, recently many researches have been studied for PT instead of wire-type transformers using cores of conventional ferrite, strongly required the efficiency improvement and miniaturization of CCFL inverters for LCD back light of notebook computers. There are 15 manufacturing industries for PT in Japan,

*To whom all correspondence should be addressed. E-mail: kjlim@chungbuk.ac.kr

taking the most technical lead in this field. Their PTs were used for LCD back light inverters of PDA, DVD players, car navigation system, camcorder, digital camera and notebook computers, and their capacities were around 10–50 W [2, 3]. PT is possible to make step-up and step-down voltages with the structure designs of vibration modes as in wire type transformers. Main applications of step-down PTs may be expected the various adaptors, ac-dc converter and dc-dc converter, etc. The development and commercial use of step-down PTs are later than those of step-up PTs. The reason was that the requirement in a market for step-down PTs was weak relatively and it was difficult to product due to the complicated structure as compared with step-up PTs. Furthermore, the internal impedance and output impedance of step-up PTs are high generally, but step-down PTs are low. Therefore, even if the primary and secondary elements of step-up PT are exchanged each other, it can not be used as a step-down PT [4].

This paper proposes a step-down PT that has the turn rate of 10:1 and the output power of 10 W for the charger and adaptor of mobile phones, expecting the largest demand of various applications. The design of this transformer adopts the multi-layer method using a thickness extensional vibration mode for low impedance. Piezoelectric ceramic of step-down PT has the ternary composition as a modified PZT. In order to satisfy the optimal conditions for multi-layer ceramic processes, it is experimented by changing the various processing parameters such as composition ratio of starting materials, milling condition, several kinds of organic binders, organic solvents, press methods, sintering conditions, and polarization methods.

Microstructure and crystallinity of the ceramic were analyzed by SEM and XRD. Piezoelectric characteristics in low electric field range were estimated by impedance analyzer and Berlincourt d_{33}-meter, and those in high electric field were measured by laser vibrometer. The input and output structures such as optimal size and number of multi-layer in step-down PT are composed by finite element analysis (FEA) and design method obtained from measurement result of material properties in the electromechanical equivalent circuit. From the results of two methods, PT is the multi-layer types having multiple piezoelectric layer, insulation and electrode layer, and uses a thickness extensional vibration mode. The selection of internal electrode material is so important, and it will be chosen considerably with the sintering temperature of ceramic processes. PT is great different from the conventional winding transformer in operating method. Because the operating frequency at maximum efficiency of PT with the variations of temperature and electrical load is changed, the operating circuit with complete functions for treating these defects is required. The input and output conditions such as step-down voltage, efficiency and capacity of PT with the parameters of voltage, frequency, load, and temperature are analyzed for the optimal operating method. Finally, to examine the applications of step-down PT, an adaptor is designed and its properties are investigated.

2. Fabrication and Characteristic of PT

2.1. Ceramic Composition

Piezoelectric ceramic for high power device like PT requires material having high electromechanical coupling factor, high piezoelectric strain constant, high mechanical quality factor, high Curie temperature and low dielectric loss coefficient [5, 6]. However, it is considered necessarily that great problems are caused by the decline of mechanical quality factor with increasing temperature under high power operation of PT and Curie temperature with small change of ceramic composition [7].

In this paper, $PbZrTiO_3$-$Pb(Mn_{1/3}Nb_{2/3})O_3$ (so called PZT-PMN) ceramic with excellent piezoelectric and dielectric properties was chosen. Moreover, $Pb(Sb_{1/2}Nb_{1/2})O_3$ having high mechanical quality factor and Curie temperature is added to PZT-PMN. It is to prevent the low Curie temperature and mechanical quality factor in perovskite PZT-PMN ceramic. The exact composition formula of ternary piezoelectric ceramics is as following:

$$y\mathrm{Pb}(\mathrm{Zr}_x\mathrm{Ti}_{1-x})\mathrm{O}_3 - (1-y)\mathrm{Pb}(\mathrm{Mn}_{1/3}\mathrm{Nb}_{1/3}\mathrm{Sb}_{1/3})\mathrm{O}_3 \quad (1)$$

where, $0.45 < x < 0.52$, and $y = 0.90, 0.95$

2.2. Experimental

Table 1 shows the material properties of each ceramic compound oxide used in this experiment.

Piezoelectric ceramics were produced by the conventional mixed oxide process. After the powders were weighed in appropriate proportions with the above

Table 1. Properties of raw material.

Compounds	Purity (%)	M.P. (°C)	B.P. (°C)
PbO	99.7	886	1,480
TiO_2	99.9	1,840	3,000
ZrO_2	99.9	2,720	5,000
MnO	99.99	2,830	3,600
Nb_2O_5	99.9	1,485	–
Sb_2O_3	99.99	1,560	–

chemical formula, they were mixed and crushed for 24 hrs in a ball mill, and then dried completely in oven at 120°C. They were calcined at 750°C for 4 hrs in zirconia-covered crucible. After the calcined powders were ground by ball milling for 24 hrs again, the PVB solution of 2 wt% was mixed with the ceramic powders, and then they were pressed in the moulder of 15 mm diameter at 2 ton/cm^2 pressure. The pressed ceramic disk contains organic solution PVB, and, therefore, it burned out the organic binder. During the sintering process, the crucible was sealed to prevent the volatilization of PbO.

A variety of ceramic weight with temperature changes is measured to find the pertinent temperature for the burning-out process of organic binder. Figure 1 shows thermal gravitation analysis (TGA) with changing temperatures.

The weight with an increase of temperature reduces with regular slope up to 250°C. It seems to be caused by the evaporation of water included in ceramic disk. From 250 to 450°C, the weight declines continuously. But it does not change over 450°C. The reason is that organic solution in film combines with oxygen in the atmosphere and then CO and CO_2 formations are evaporated. The reduction of total weight is around 2% at 450°C temperature and this result almost seems to be corresponding with the PVB solution of 2 wt%. The ceramic films were sintered in a magnesia-covered crucible at 1050–1250°C for 4 hrs. The films were poled under the electric field of 3 kV/mm in silicon oil at 120°C. This poling process kept for 24 hrs at 120°C to prevent the deterioration due to space charges formed in grain boundary.

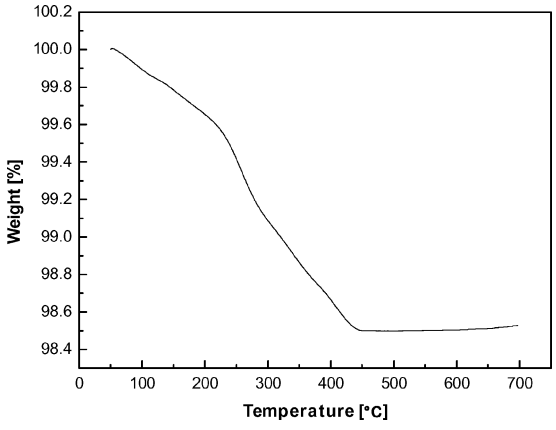

Fig. 1. Thermal gravitation analysis.

Crystalline structure of PZT-PMNS ceramics was analyzed in the 2θ ranges of 20°–70° by XRD (Cu-Kα; SCINTAG Co.). The microstructure with the changes of sintering temperature was investigated by SEM (S-2500C, HITACHI Co.). The disk-type films with 1 mm thickness and 12 mm diameter produced under the provision of EMAS 6001. Their dielectric and piezoelectric properties were measured under the low electric field. The piezoelectric strain constant was estimated by Berlincourt d_{33}-meter (CHANNEL Co.), and other piezoelectric characteristics were measured by impedance analyzer (HP 4194A).

Ferroelectric ceramics have Curie temperature that shifts from ferroelectric phase to paraelectric phase with the change of temperature, and the permittivity has a peak at Curie temperature. In order to measure Curie temperature, the poled films fixed on holder in furnace, and the changes of capacitance were estimated with temperature by impedance/gain analyzer (HP 4194A). The thermocouple contacted on surface of ceramic film to measure possibly exact capacitance, and the rising velocity of temperature controlled below 1.5°C /mm to reduce noises that could be caused by the increasing temperature.

2.3. *Results and Discussion*

2.3.1 XRD Analysis. The piezoelectric and dielectric properties of PZT family ceramics present the most excellent values at morphotropic phase boundary that coexists the tetragonal phase of Ti-rich region and rhombohedral phase of Zr-rich region together. The crystalline orientations that dipoles can rearrange in polarization process are various in the morphotropic phase boundary, and, therefore, the rearrangement of domain is ease. In order to find the morphotropic phase boundary in $yPb(Zr_xTi_{1-x})O_3 - (1-y)Pb(Mn_{1/3}Nb_{1/3}Sb_{1/3})O_3$ ceramics, XRD analysis is carried out as parameters of x and y.

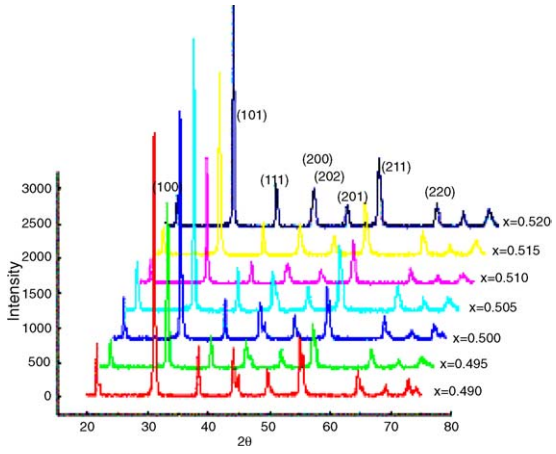

Fig. 2. XRD patterns as a function of x in $0.95Pb(Zr_xTi_{1-x})O_3 - 0.05Pb(Mn_{1/3}Nb_{1/3}Sb_{1/3})O_3$ ceramics.

Figures 2 and 3 show XRD patterns with a function of x at y parameters of 0.95 and 0.90, respectively. All peaks of XRD patterns in Figs. of 2 and 3 exhibit typical perovskite structure without the secondary phases like pyrochlore. It indicates that the splitting of (200) and (002) in tetragonal phase reduces gradually with the increasing x and disappears completely at $x = 0.505$ in $y = 0.95$ of Fig. 2, and the patterns of rhombohedral phase show finally.

From this results, it can know that the phase transition occurs between $x = 0.505$ and 0.510.

Also, the splitting patterns of tetragonal phase disappear at $x = 0.500$ in $y = 0.90$ of Fig. 3 and the rhombohedral phase show. Therefore, it is considered that the phase transition of PZT-PMNS ceramics in $y = 0.90$ is generated at $x = 0.500$.

2.3.2 SEM Analysis. The microstructures of SEM are measured with the change of sintering temperature at $y = 0.95$, $x = 0.505$ and $y = 0.90$, $x = 0.500$ in composition of $yPb(Zr_xTi_{1-x})O_3 - (1 - y)Pb(Mn_{1/3}Nb_{1/3}Sb_{1/3})O_3$ ceramics. It indicates that the grain size of PZT-PMNS grows slightly with the increasing temperature. The grain boundary should be dense and uniform in piezoelectric devices like PTs and, also, it is required the high-density material without pore [8]. The grain growth of sintered films does not achieve completely at 1100°C, but the grain formation achieves at 1150°C and shows dense structure without pore. The grain size is about 2–3 μm and uniform. At above 1200°C, the grain boundary grows completely and, however, goes to be non-uniform. It indicates that the pore appears slowly at 1250°C and the grain is weakened mechanically. Therefore, it concludes that the optimal sintering temperature of PZT-PMNS ceramics is 1150°C at $x = 0.505$ and $y = 0.95$. On the other hand, the optimal temperature in ceramic composition of $x = 0.500$ and $y = 0.90$ is 1200°C.

2.3.3 Piezoelectric and Dielectric Properties with Composition Change. Figure 4 shows the electromechanical coupling factor, k_p, with functions of x and y in the composition of PZT-PMNS ceramics. The sintering temperature in this figure is 1150°C at $y = 0.95$ and 1200°C at $y = 0.90$. The variation of k_p in a function

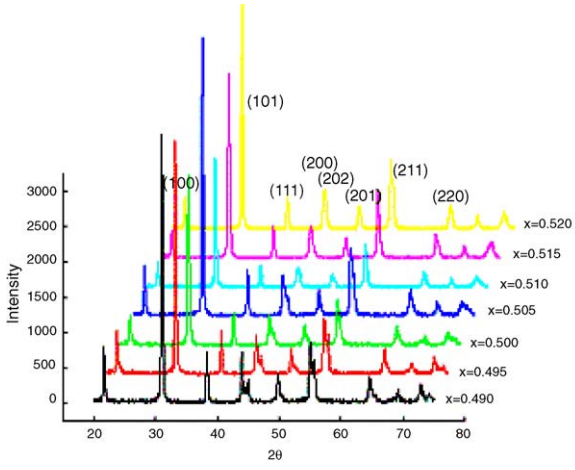

Fig. 3. XRD patterns as a function of x in $0.9Pb(Zr_xTi_{1-x})O_3 - 0.1Pb(Mn_{1/3}Nb_{1/3}Sb_{1/3})O_3$ ceramics.

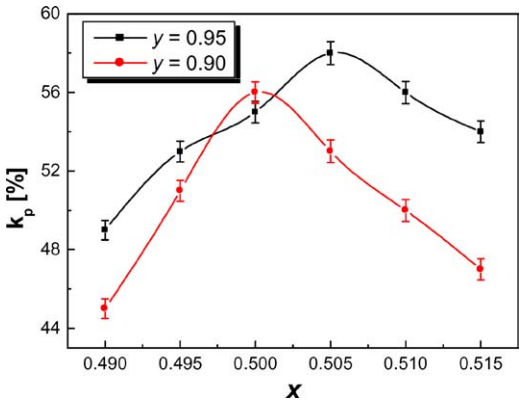

Fig. 4. The change of kp as a function of x and y in $yPb(Zr_xTi_{1-x})O_3 - (1 - y)Pb(Mn_{1/3}Nb_{1/3}Sb_{1/3})O_3$ceramics.

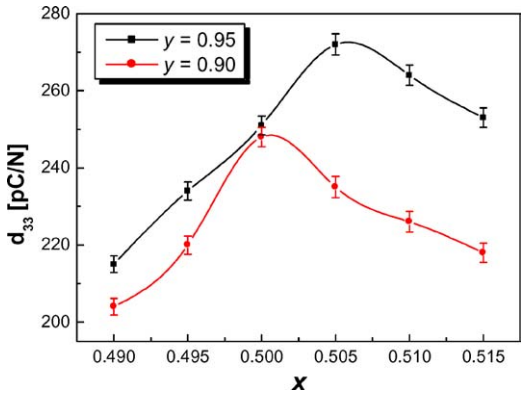

Fig. 5. The change of d_{33} as a function of x and y in $y\mathrm{Pb}(\mathrm{Zr}_x\mathrm{Ti}_{1-x})\mathrm{O}_3 - (1-y)\mathrm{Pb}(\mathrm{Mn}_{1/3}\mathrm{Nb}_{1/3}\mathrm{Sb}_{1/3})\mathrm{O}_3$ ceramics.

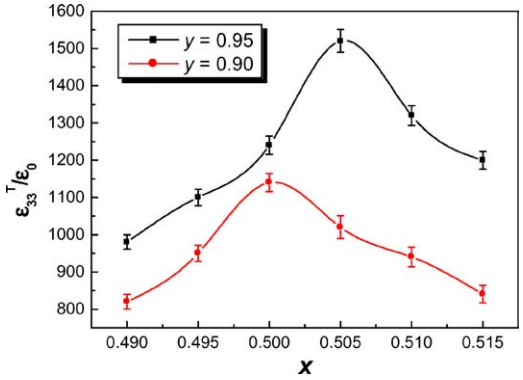

Fig. 7. The change of $\varepsilon_{33}^T/\varepsilon_0$ as a function of x and y in $y\mathrm{Pb}(\mathrm{Zr}_x\mathrm{Ti}_{1-x})\mathrm{O}_3 - (1-y)\mathrm{Pb}(\mathrm{Mn}_{1/3}\mathrm{Nb}_{1/3}\mathrm{Sb}_{1/3})\ \mathrm{O}_3$ ceramics.

of x shows convex shape for y of 0.9 and 0.90, respectively. The maximum value of k_p in $y = 0.95$ is 58% at $x = 0.505$ and that in $y = 0.90$ is 56% at $x = 0.500$. Figures 5 and 6 exhibit piezoelectric strain constant, d_{33}, and mechanical quality factor, Q_m, with functions of x and y, respectively. The curves of d_{33} and Q_m^{-1} as a function of x are similar to the k_p trend in Fig. 4. It means that the composition of PZT-PMNS ceramics exists in the morphotropic phase boundary (MPB) region when x is of 0.505 and 0.500 at $y = 0.95$ and 0.90, respectively. These results agree intimately with x and y values that are generated the phase transition from XRD analysis. Because the tetragonal phase and rhombohedral phase coexist in morphotropic phase boundary, the rearrangement of domain is easy for polarization process and, therefore, strong piezoelectric properties are able to obtain.

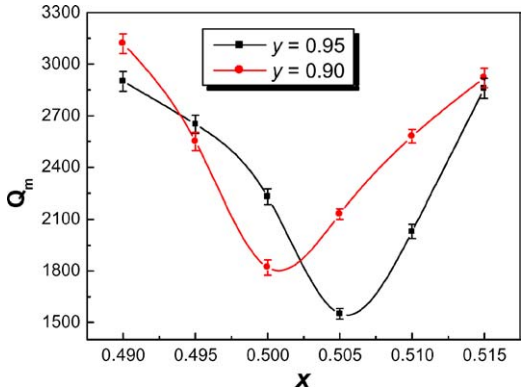

Fig. 6. The change of Q_m as a function of x and y in $y\mathrm{Pb}(\mathrm{Zr}_x\mathrm{Ti}_{1-x})\mathrm{O}_3 - (1-y)\mathrm{Pb}(\mathrm{Mn}_{1/3}\mathrm{Nb}_{1/3}\mathrm{Sb}_{1/3})\mathrm{O}_3$ ceramics.

It exhibits a tendency that piezoelectric and dielectric properties decrease and mechanical quality factor increases, growing up the dopants of ternary PMNS. It means that the pinning effect is generated by Mn^{2+} and Mn^{3+}, added in ternary PMNS, and the shift of domain wall is suppressed. Hence, the piezoelectric properties reduce and mechanical quality factor increases [9].

Figure 7 shows the changes of permittivity, $\varepsilon_{33}^\mathrm{T}/\varepsilon_0$, as functions of x and y in the composition of PZT-PMNS ceramics. Also, the curve shape of permittivity exhibits the similar trend of k_p, d_{33} and Q_m^{-1}. This convex trend is explained by the behavior of MPB region. Figure 8 shows the changes of permittivity as a function of temperature, which is measured in MPB region by dielectric temperature analysis (DTA). The permittivty curve goes slowly up with the increasing temperature, and then exhibits a peak value at a special temperature. After peak point, its curve reduces abruptly. This

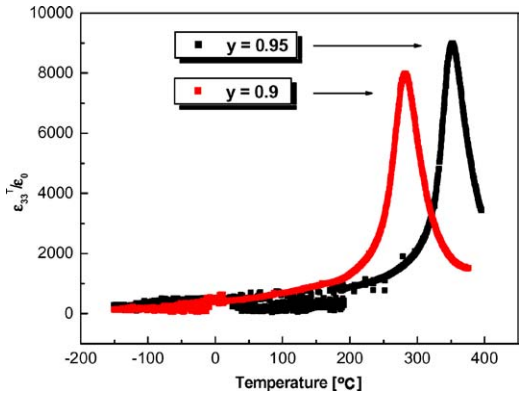

Fig. 8. Phase transition temperature by DTA.

Table 2. The properties of piezoelectric ceramic compositions.

	k_p (%)	Q_m	Curie temp. [°C]
0.95PZT-0.05PMN	60	1000	320
0.95PZT-0.05PMNS	58	1520	350

peak point is the phase transition temperature that is one of some specific features in ferroelectric ceramics and transfers from ferroelectric phase to paraelectric phase; that is, called Curie temperature. It indicates that Curie temperature is around 350°C at $y = 0.95$ and 290°C at $y = 0.90$ as shown in figure. The Curie temperature at $y = 0.95$ reduces about 60°C, comparing that at $y = 0.90$. It is considered that Curie temperature reduces with the increasing PMNS dopants, because Curie temperature of PZT in basic compositions is lower than that of ternary PMNS.

Table 2 shows the properties of PZT-PMNS ceramics, compared with properties of PZT-PMN ceramics. The k_p of 0.95PZT-0.05PMNS composition is lower about 2% than that of 0.95PZT-0.05PMN, and Q_m and Curie temperature, which are key factors in temperature rising rate of high power piezoelectric devices, increase around 50% and 10%, respectively. From these results, it is expected that piezoelectric PZT-PMNS ceramic may be available for high power piezoelectric devices such as PT and ultrasonic motor.

3. Formation and Characteristics of PT

3.1. PT Fabrication

PTs are produced using the developed piezoelectric ceramics and internal electrodes of Pd-Ag paste. After the above mentioned ceramics calcinated and then crushed, the powder was mixed with organic solution and the green sheet was produced by doctor blade method. The internal electrode layers were located in each green sheet, and then pressed. The prepared multi-layer films sintered in electrical furnace. After Ag electrodes were prepared on both side of films, the input and output parts was polarized. All processing conditions were same with the ceramic formation parameters such as sintering temperature and time, pressing pressure, polarization temperature, and electric field, etc. Figure 9 shows the construction of PT. It is consisted of input layer, insulation layer and output layer. The polarizing direction of primary and secondary part in PTs is

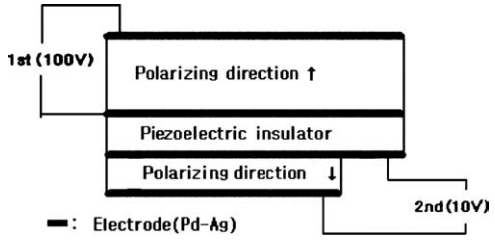

Fig. 9. Fabricated PT.

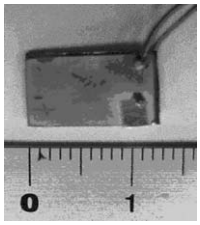

Fig. 10. Photography of fabricated PT.

reversing each other. Figure 10 displays the practical picture of PT, prepared in this experiments, and its size is $12 \times 10 \times 1.3$ mm^3.

3.2. Characteristic Analysis and Design of PT

To analyze PTs characteristics, the distributed-constant equivalent circuit or lumped-constant equivalent circuit can be used. The lumped-constant equivalent circuit is generally easier than the distributed-constant equivalent circuit. The element values of lumped-constant equivalent circuit can be measured by impedance analyzer, which uses those near the resonant frequency. Figure 11 shows the lumped-constant equivalent circuit of PTs. PTs characteristics from Fig. 11 can induce the following relation equations.

$$G = \frac{E_2}{E_1} \tag{2}$$

$$\eta = \frac{P_2}{P_1} \tag{3}$$

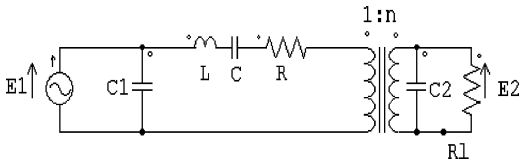

Fig. 11. Equivalent circuit for piezoelectric transformer.

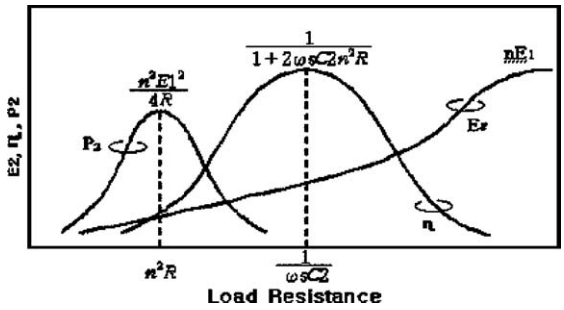

Fig. 12. Calculated load characteristic for the piezoelectric transformer.

where, G is voltage gain, E_1 and E_2 are input and output voltage, P_1 and P_2 are input and output power, respectively.

The characteristics of gain G, output power P_2, and efficiency η are calculated by the above equations and shown in Fig. 12. Figures 13 and 14 the calculated characteristics for gain and efficiency as a function of frequency at load resistance of 10 Ω for PTs, developed in this experiment.

The maximum peak of gain G near 0.85 MHz is the first mode for thickness extensional vibration. The peak of second mode occurs at 1.7 MHz. The efficiency of 92% is obtained near the second mode. Furthermore, the efficiency exhibits higher than 90% at the frequency ranges between 0.7 MHz and 2.8 MHz. It shows that the characteristics of G and η is possible to be controlled by frequency modulation.

3.3. Performance Estimation of PTs

In order to measure the properties of PT, the measuring systems are consisted by a function generator, power amplifier, oscilloscope, and variable load. The variable frequency generated using a function generator (HP 4173) is amplified by signal power amplifier (NF 401), and is applied to input terminal of PT. The load is no-induction variable resistance of maximum 1.5 kΩ. The current and voltage in electric input and output are measured using current probe (Tek. 6015A) and voltage probe (Tek. 3015). The self-temperature that occurs from the operation of PT is measured by non-contacted type infrared thermometer (INF 100).

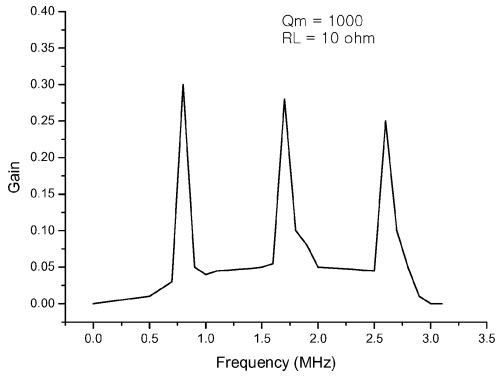

Fig. 13. Calculated characteristic for gain G.

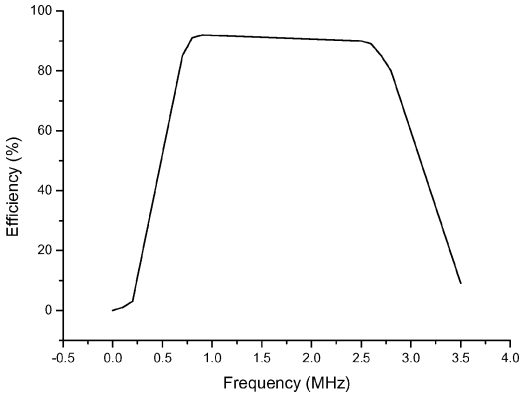

Fig. 14. Calculated characteristic for efficiency η.

Figure 15 shows the measured admittance as a function of frequency at the primary part, as the output terminals of secondary part are shorted. The resonant frequency exhibits at 1.7 MHz.

Figures 16 and 17 show gain G and efficiency η with the changes of load resistance. The measured frequency was obtained in this measurement, as the gain becomes to maximum for each R_L value. The gain G

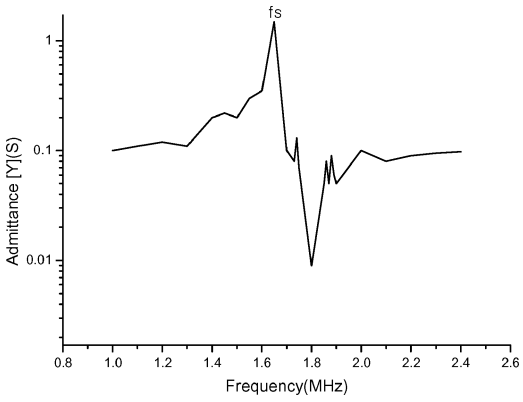

Fig. 15. Measured input admittance characteristic for piezoelectric transformer.

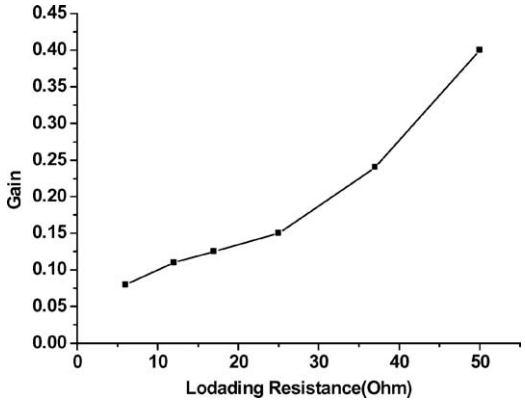

Fig. 16. Measured gain G load characteristic for piezoelectric transformer.

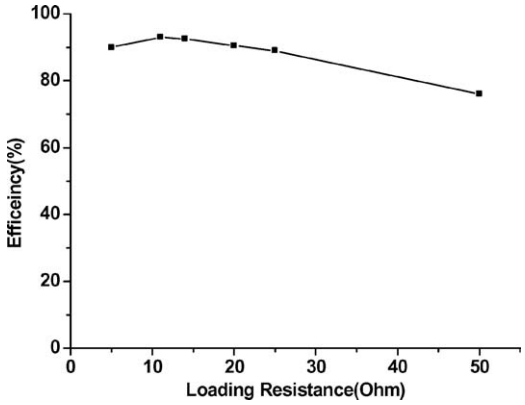

Fig. 17. Measured efficiency η load characteristic for piezoelectric transformer.

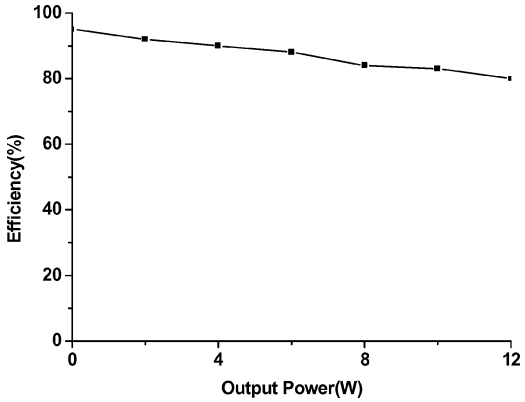

Fig. 18. Measured efficiency—output power characteristic for piezoelectric transformer.

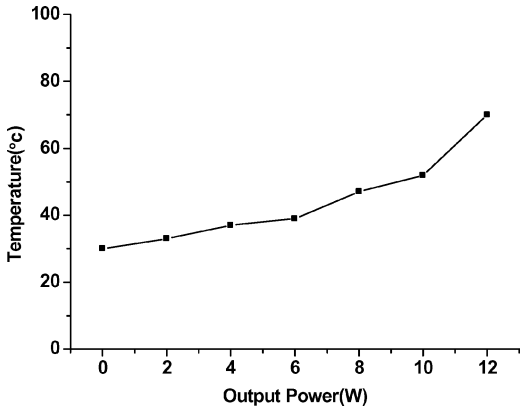

Fig. 19. Measured surface temperature characteristic for piezoelectric transformer.

is 0.13 at the load resistance of 10 Ω. The gain increases gradually with the increasing load resistance. The maximum efficiency is 94% at load resistance of 12 Ω, and the efficiency shows greater than 80% at the ranges of R_L from 5 to 50 Ω. From Eqs. (1) and (2), the calculated value of maximum efficiency is 95% at load resistance of 8.2 Ω. There is a little difference between the calculated value and measured one. The reasons are due to the changes of resonant frequency with the variation of R_L, and the changes of equivalent circuit values between small voltage operation and high voltage operation.

The turn ratio is 0.1 in the prepared step-down PTs and the efficiency is 92%. Figures 18 and 19 show the efficiency and surface temperature characteristics of PTs as a function of output power at load resistance of 10 Ω. As output power increases, it shows that the efficiency reduces and the surface temperature increases. It indicates that the efficiency is 90% at 10 W and the temperature of PTs is about 50°C. The utilizing conditions of commercial PTs generally set on the basis of rising temperature, which standardizes 20°C. Comparing the electromagnetic transformer, it is considered that the designed PTs have excellent performances at standpoints of efficiency and energy density.

4. Application as an Adaptor

High frequency switching is an effective method to miniaturize dc-dc converter, but there is a fault that the switching loss is increased. In order to reduce the switching losses in high frequency switching,

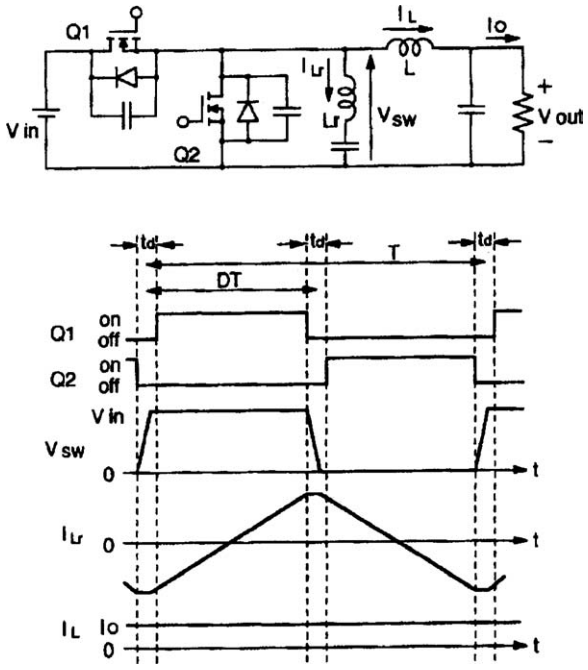

Fig. 20. Single-ended type ZVS-CV dc-dc converter with a commutation inductor.

zero-voltage or zero-current switching methods are proposed. However, the resonant converters using these methods have a large stress in switching devices. To overcome the switching losses, the zero-voltage-switching, clamped-voltage (ZVS-CV) has been presented as shown in Fig. 20. It takes this concept for granted that a winding-type magnetic transformer as a step-down transformer is used. Figure 20 shows a single-ended type ZVS-CV dc-dc converter using the aided-mutual inductor, L_r, and a large capacitor in series connection. The current I_L of output inductor is constant approximately due to the large L, but the waveform of mutual inductor current I_{Lr} is a triangle wave, which is changed from positive to negative.

The magnetizing current to realize ZVS is explained by the mutual inductor in this case. The output voltage is controlled generally by PWM with a constant switching frequency. In this experiment, the dc-dc converter circuit of PTs operating in several MHz ranges applies a ZVS-CV switching topology and designs as shown in Fig. 21. Figures 22 and 23 show the output power and efficiency as a function of frequency with circuit parameters as following: $L_r = 8.8\ \mu$H, $L_P = 30\ \mu$H, $L = 0.147$ mH, C = 46 pF, $R = 7.4\ \Omega$, $C_{d1} = 429$ pF, $C_{d2} = 9754$ pF, and turn ratio = 0.19.

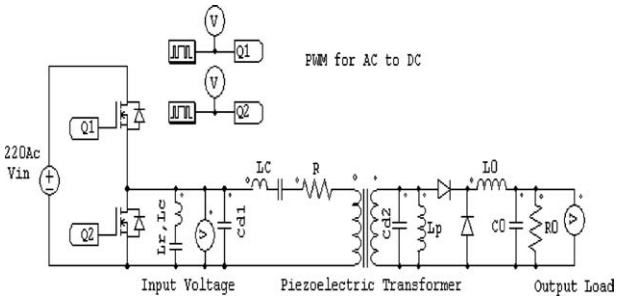

Fig. 21. ZVS-CV dc-dc converter with piezoelectric transformer.

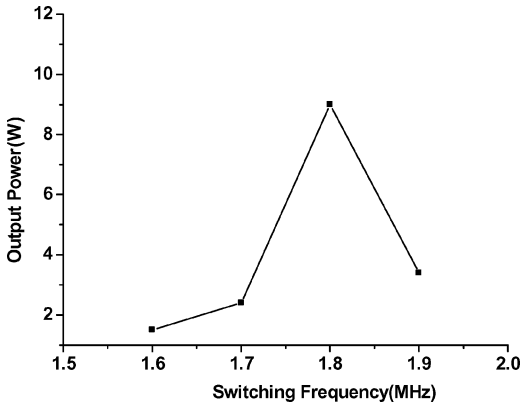

Fig. 22. Calculated switching frequency characteristics of output power in an adaptor.

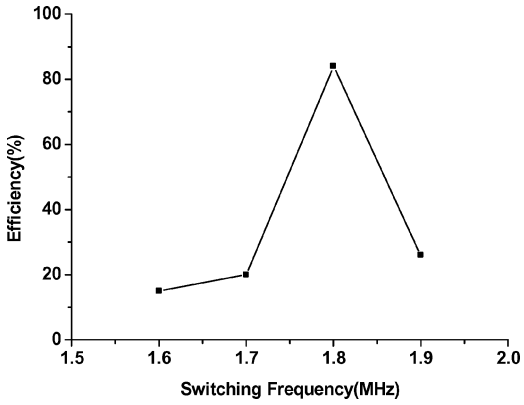

Fig. 23. Calculated switching frequency characteristics of efficiency in an adaptor.

The maximum output power is about 10 W and efficiency is 85% at the switching frequency of 1.8 MHz. It exhibits a little different result between the calculated value and the measured value of PTs characteristics

under the above-mentioned conditions. The efficiency of PTs has more excellent value than that of general adaptor using the electromagnetic transformer. The PTs developed in this research are possible to apply for dc-dc converters or adaptors of 10 W class.

5. Conclusion

PTs have several merits in comparison with the electromagnetic transformer, and are used as a step-up transformer for high voltage and low current types. Therefore, the application extents of PTs become wider. However, it does not be commercialized in the step-down transformer that is required as a dc power supply such as dc-dc converter and adaptor. In order to develop the step-down PTs of 10 W class and turn ratio of 0.1 with high efficiency and miniaturization, the piezoelectric ceramics and PTs designs are estimated with a variety of characteristics.

The basic composition of piezoelectric ceramics consists of ternary $y\mathrm{Pb}(\mathrm{Zr}_x\mathrm{Ti}_{1-x})\mathrm{O}_3$-$(1-y)$ $\mathrm{Pb}(\mathrm{Mn}_{1/3}\mathrm{Nb}_{1/3}\ \mathrm{Sb}_{1/3})\mathrm{O}_3$. In the piezoelectric characteristics evaluations, at $y = 0.95$ and $x = 0.505$, the electromechanical coupling factor(k_p) is 58%, piezoelectric strain constant(d_{33}) is 270 pC/N, mechanical quality factor(Q_m) is 1520, permittivity($\varepsilon_{33}^T/\varepsilon_0$) is 1500, and Curie temperature is 350°C. At $y = 0.90$ and $x = 0.500$, k_p is 56%, d_{33} is 250 pC/N, Q_m is 1820, $\varepsilon_{33}^T/\varepsilon_0$ is 1120, and Curie temperature is 290°C. It shows the excellent properties at morphotropic phase boundary regions. It exhibits that piezoelectric and dielectric properties decrease and mechanical quality factor increases, as the dopants of ternary PMNS increase. It means that the pinning effect is generated by addition of Mn in ternary PMNS. The k_p of 0.95PZT-0.05PMNS composition proposed in this research is lower about 2% than that of 0.95PZT-0.05PMN, and Q_m and Curie temperature increase around 50% and 10%, respectively. From these results, it is expected that piezoelectric PZT-PMNS ceramic may be available for high power piezoelectric devices such as PTs.

The design of step-down PTs for adaptor proposes a multi-layer structure to overcome some structural defects of conventional PTs. In order to design PTs and analyze their performances, the finite element analysis and equivalent circuit analysis method are applied. The step-down PTs are produced with a multi-layer structure, which uses the evaluated piezoelectric ceramics and has the designed geometric size. The maximum peak of gain G as a first mode for thickness extensional vibration occurs near 0.85 MHz at load resistance of 10 Ω. The peak of second mode at 1.7 MHz is 0.12 and the efficiency is 92%.

In order to investigate the applications of designed PTs, the zero-voltage-switching, clamped-voltage (ZVS-CV) topologies are introduced and step-down PTs for an adaptor are designed and simulated. From the calculated results, the output power is about 10 W and efficiency is 85% at the switching frequency of 1.8 MHz. The efficiency of adaptor with PTs has more excellent value than that with the electromagnetic transformer. The PTs developed in this research has the capacity of 10 VA, turn ratio of 0.1 and above efficiency 90%, and are possible enough to apply for dc-dc converters or adaptors.

References

1. T. Futakuchi et al., *Jpn. J. Appl. Phys*., **38**, 3596 (1999).
2. D.O. Hur et al., in *Proc. of 5th ICPADM*, 843 (1997).
3. B. Koc, S. Alkoy, and K. Uchino., *1999 IEEE Ultrasonics Symposium*, 931 (1999).
4. H. Fukunaga et al., in *Proc. of '98UFFC*, 1504 (1998).
5. J.H. Kim et al., *IEEE Trans. on Circuits and Systems*, **42**, 307 (1995).
6. S. Priya, K. Uchino, J. Ryu, H, Luo, and D. Viehland, *Ferroelectrics*, **274**, 299 (2002).
7. S. Hirose et al., in *Proc. of '98Ultrasonic Symposium*, 953 (1998).
8. S. Kawashima et al., in *Proc. of '94Ultrasonic Symposium*, 525 (1994).
9. M. Imori et al., *IEEE Trans. on Nuclear Science*, **45**, 777 (1998).